Method for Predicting f_T for Carbon Nanotube FETs

Leonardo C. Castro, D. L. John, *Student Member, IEEE*, D. L. Pulfrey, *Fellow, IEEE*, Mahdi Pourfath, Andreas Gehring, *Member, IEEE*, and Hans Kosina, *Member, IEEE*

***Abstract*—A method based on a generic small-signal equivalent circuit for field-effect transistors is proposed for predicting the unity–current–gain frequency f_T for carbon-nanotube devices. The key to the useful implementation of the method is the rigorous estimation of the values for the components of the equivalent circuit. This is achieved by numerical differentiation of the charges and currents resulting from self-consistent solutions to the equations of Schrödinger and Poisson. Sample results are presented, which show that f_T can have a very unusual dependence on the gate–source bias voltage. This behavior is due mainly to the voltage dependence of the transconductance and capacitance in the presence of quasi-bound states in the nanotube.**

***Index Terms*—Carbon nanotube transistors, field-effect transistors (FETs), nanotechnology, quantum effect semiconductor devices, quantum wires, semiconductor device modeling, small-signal analysis.**

I. Introduction

CARBON-NANOTUBE field-effect transistors (CNFETs) are being seriously considered for meeting the requirements of the 11-nm technology node [1]. Their dc performance is predicted to be superior to that of ultimately scaled silicon MOSFETs [2], [3], and impressive values for drain current and transconductance have already been reported in prototype devices [4]. The ac capabilities of CNFETs are not yet so obvious. Thus far, measurements on laboratory devices have been limited by experimental difficulties and parasitics [5]–[7]. Thus, the highest reported frequency of 580 MHz, for operation without signal degradation, cannot be viewed as a representative value for an intrinsic device.[1] One way to investigate the ac capabilities of CNFETs would be to perform ac simulations with the same rigour that has characterized earlier dc simulations [9], [10]. This means using a self-consistent Schrödinger–Poisson solver to compute values for the parameters appearing in, for example, a small-signal equivalent circuit, from which a useful metric, such as f_T, could be obtained. Through the use of this self-consistent procedure, we expect a more accurate result than that predicted in [11], where capacitances in the equivalent-circuit model were computed assuming a metallic nanotube and electrostatics for an infinitely long coaxial system.

In this paper, we perform a rigorous calculation of the gate–voltage dependencies of both the transconductance [12], [13] and the capacitances, including the so-called "quantum capacitance" [13], in order to compute the small-signal equivalent-circuit parameters from which our improved estimates of f_T for CNFETs are obtained. This analysis reveals a bias dependence that is quite unusual, and which may prove useful in voltage-controlled high-frequency circuitry.

II. Small-Signal Model

A. Equivalent Circuit

Starting from Maxwell's first two equations, and considering a system with three electrodes, through which charge can enter or leave the system, it follows that

$$\frac{\partial Q}{\partial t} = \frac{\partial Q_S}{\partial t} + \frac{\partial Q_D}{\partial t} + \frac{\partial Q_G}{\partial t} = 0 \tag{1}$$

where Q is the total charge within the system and Q_S, Q_D, and Q_G refer to charges associated with each of the device's three terminals, namely: 1) the source; 2) drain; and 3) gate, respectively. Labeling displacement currents with a superscript d, it follows from (1) that

$$i_s^d + i_d^d + i_g^d = 0 \tag{2}$$

where the lower case subscripts indicate that we are going to be dealing with small-signal parameters. This notation is used also for the voltages, e.g., the total gate voltage v_G comprises a dc voltage V_G and an ac small-signal v_g. If we suppose that Q_S, Q_D, and Q_G are functions of time through the application of time-dependent voltages $v_S(t)$, $v_D(t)$, and $v_G(t)$, then each displacement current will comprise three terms, e.g.,

$$i_g^d = -C_{GS}\frac{\partial v_S}{\partial t} - C_{GD}\frac{\partial v_D}{\partial t} + C_{GG}\frac{\partial v_G}{\partial t} \tag{3}$$

where the capacitances come from the set

$$C_{ij} = \mp\frac{\partial Q_i}{\partial v_j}, \qquad i,j = S,D,G \tag{4}$$

where the minus sign is taken when $i \neq j$, and the plus sign is taken when $i = j$ [14]. Not all the capacitances in this set are independent, and it can be easily shown that, e.g.,

$$C_{GG} = (C_{GS} + C_{GD}) = (C_{SG} + C_{DG}). \tag{5}$$

Manuscript received April 23, 2005; revised July 7, 2005.

L. C. Castro, D. L. John, and D. L. Pulfrey are with the Department of Electrical and Computer Engineering, University of British Columbia, Vancouver, BC V6T 1Z4, Canada (e-mail: pulfrey@ece.ubc.ca).

M. Pourfath and H. Kosina are with the Institute for Microelectronics, Technical University of Vienna, A-1040 Vienna, Austria.

A. Gehring was with the Institute for Microelectronics, Technical University of Vienna, A-1040 Vienna, Austria. He is now with AMD Saxony, 01109 Dresden, Germany.

Digital Object Identifier 10.1109/TNANO.2005.858603

[1]Very recently, operation up to 10 GHz has been reported [8], albeit with considerable signal attenuation.

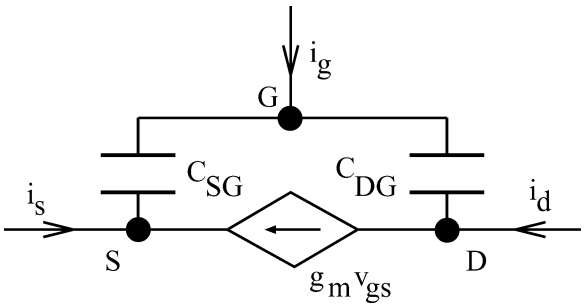

Fig. 1. Small-signal equivalent circuit for the total ac currents under the condition that only the potential on the gate is time-dependent.

Thus, if we now consider v_S and v_D to be held constant, as is appropriate for an estimation of f_T in the absence of parasitic source and drain resistances, then it follows that

$$i_g^d = (C_{SG} + C_{DG})\frac{\partial v_{GS}}{\partial t}. \tag{6}$$

This displacement current, which is also the total gate current i_g, can be computed from an equivalent circuit, such as is shown in Fig. 1.

Turning now to the conduction currents, we employ the standard quasi-static approach for a current that depends on two potential differences, i.e., in this case, v_{GS} and v_{DS}. In its linear implementation, this leads to a drain conduction current of

$$i_d^c = g_m v_{gs} + g_{ds} v_{ds}. \tag{7}$$

Here, as we are keeping v_{DS} constant, the term involving the output conductance g_{ds} need not be considered.

This completes the specification of the small-signal equivalent circuit. It is a well-founded circuit with the only approximation being the use of quasi-statics to obtain linear expressions for the conduction currents. Note that the interfacial conductance of $4q^2T/h$, due to transverse-mode reduction on passing from a large many-mode electrode to a two-mode quasi-one-dimensional (1-D) nanotube with a transmission probability T [15], is not shown explicitly in Fig. 1, as it is implicit in the transconductance g_m.

On the basis of the circuit shown in Fig. 1, the common-source short-circuit unity–current–gain frequency, as extrapolated from a frequency at which the gain rolls off at -10 dB/decade, is given by

$$f_T = \frac{g_m}{2\pi(C_{SG} + C_{DG})}. \tag{8}$$

B. Model Parameters

In order to relate C_{SG} and C_{DG} to meaningful physical quantities, we firstly split the charges Q_S and Q_D into the following two components:

$$\begin{aligned} Q_S &= Q_{\rm SE} + Q_{ST} \\ Q_D &= Q_{\rm DE} + Q_{DT} \end{aligned} \tag{9}$$

where $Q_{\rm SE}$ and $Q_{\rm DE}$ are charges on the actual source and drain electrodes, respectively; and Q_{ST} and Q_{DT} are charges on the nanotube that enter via the source and drain electrodes, respectively. Each of these charges is supplied by the appropriate displacement current, as illustrated in Fig. 2. A capacitance can now be related to each of the charge components. For the source capacitance, for example, we have

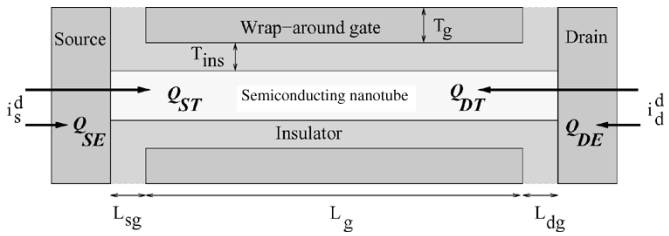

Fig. 2. Charge supply to and through the source and drain electrodes in a coaxial CNFET.

$$C_{SG} = -\frac{\partial Q_S}{\partial v_G} = -\frac{\partial Q_{\rm SE}}{\partial v_G} - \frac{\partial Q_{ST}}{\partial v_G} = C_{\rm SE} + C_{ST}. \tag{10}$$

These capacitive components are readily calculated because their related charges can be computed from a recently described self-consistent dc Schrödinger–Poisson solver [9]. This solver has been adapted to employ Neumann boundary conditions at the nonmetallic bounding surfaces in the structure depicted in Fig. 2. In our solver, the source- and drain-related nanotube charges Q_{ST} and Q_{DT} are computed from integrations of the line charges that are related to the wave functions associated with carriers communicating with the system via the source and drain, respectively. Wave functions are computed via the effective-mass Schrödinger equation with plane-wave solutions assumed in the metal contacts. A phenomenological band discontinuity is used to model the electrode–nanotube heterointerfaces as simple Schottky barriers. Normalization of the wave functions is achieved by setting the probability density current equal to the current expected from the Landauer equation for ballistic transport. The small-signal parameters C_{ST} and C_{DT} are computed for a given drain bias via numerical derivatives with a perturbation in the gate voltage on the order of 0.1 mV. Similarly, g_m is computed from Landauer's equation.

$C_{\rm SE}$ is associated with the change in the charge that resides on the actual source electrode $Q_{\rm SE}$. Similarly, $C_{\rm DE}$ is related to a change in $Q_{\rm DE}$. These charges are computed from appropriate applications of Gauss' Law in integral form.

III. Results and Discussion

Results are presented for a coaxial transistor structure, as shown in Fig. 2, with Schottky-barrier contacts at the source/tube and drain/tube interfaces. This embodiment, which avoids the need to dope the nanotube, and which employs the ultimate "multigate" to combat short-channel effects, is being actively pursued experimentally [16]. Here, by way of an example, we consider a $(16, 0)$ carbon nanotube with a radius of 0.63 nm, a length $L_t = 20$ nm, and a relative permittivity of 1 [17]. The insulator has a thickness $T_{\rm ins} = 2.5$ nm, and its relative permittivity is taken to be 25, as is appropriate for zirconia, which is used in some high-performance CNFETs [18]. The gate electrode is separated from the source and drain electrodes by $L_{sg} = L_{dg} = 4$ nm and has a thickness $T_g = 3$ nm. The

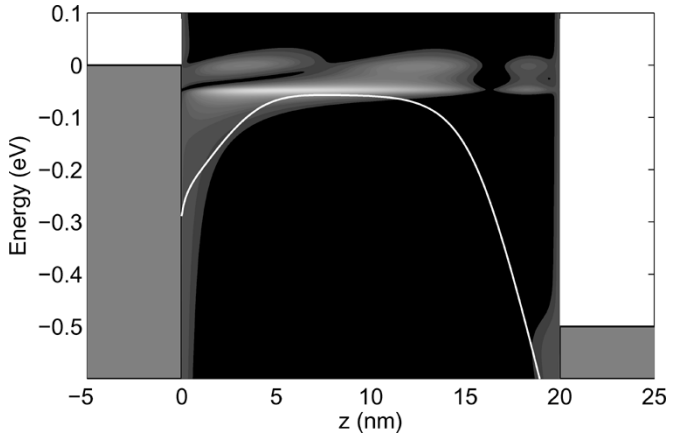

Fig. 3. Greyscale representation of the energy and position dependence of the electronic charge in the nanotube at $V_{GS} = 0.4$ V and $V_{DS} = 0.5$ V. The uniform columns to the left and right represent the energy range below the Fermi level in the source and drain, respectively. The conduction-band edge is superimposed.

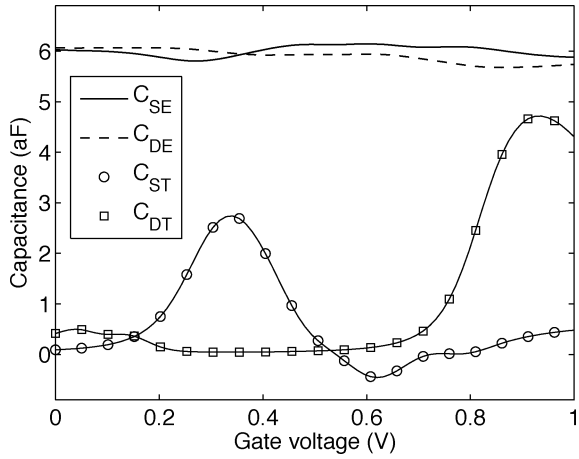

Fig. 4. Components of the source and drain capacitances.

work function of the gate is taken to be the same as that of the intrinsic nanotube (4.5 eV), whereas the source and drain metallizations have a work function of 3.9 eV. Although this yields an n-type device, inasmuch as the dominant carriers are electrons, p-type operation is directly analogous, and, owing to the symmetry of the nanotube's band structure about the midgap energy, can be obtained through the use of a higher work function metal. Thus, the CNFET considered here can be classed as a negative Schottky-barrier device, such as has been predicted to give dc characteristics that are superior to those of devices with either zero or positive Schottky barriers at the end contacts [2]. In negative-barrier CNFETs, the conduction current is due to thermionic emission at the source–tube and drain–tube interfaces. Quantum-mechanical reflection at these interfaces, due to the band discontinuities mentioned earlier, leads to resonances, and the appearance of quasi-bound states, at least in nanotubes of the short length considered here. This plays a significant role in determining the values for the model parameters discussed below. An illustrative example of the charged quasi-bound states and the conduction-band profile in the device is presented in Fig. 3. The example shows charge in the first and second quasi-bound states, and the appearance of charge in an additional quasi-bound state in the potential well at the drain end of the device.

The results presented here are intended to illustrate the ability of the proposed method to provide meaningful estimates of f_T for CNFETs. An optimization of the CNFET structure to suggest an upper bound for f_T is not attempted at this stage, but some comments are offered after the discussion of the current results as to the factors that might be important in this regard. All the results presented below are for operation at $V_{DS} = 0.5$ V.

The various components of the capacitance are shown in Fig. 4. Considering, firstly, the tube capacitance C_{ST} due to charge injected from the source, the peak at around $V_{GS} = 0.35$ V corresponds to alignment in energy of the source Fermi level and the first quasi-bound state for electrons in the nanotube [13]. The peak in C_{DT} is displaced from the peak in C_{ST} by approximately V_{DS} [13] and corresponds to alignment in energy of the drain Fermi level and the first quasi-bound state.

Considering now the capacitances associated with changes in charge on the actual end contacts, it can be seen that these are relatively bias independent. In fact, this is due to $C_{\rm SE}$ and $C_{\rm DE}$ being dominated by the regions of overlap of the end contacts with the edges of the gate electrode. Obviously, this capacitance could be reduced by increasing the separation between the end contacts and the edges of the gate, or by making the gate electrode thinner, or by making the end contacts more "needle-like" [19]. The latter could be achieved by utilizing metallic nanotubes for the source and drain. The total capacitances associated with each electrode are shown in Fig. 5(a).

We now discuss the transconductance, as shown in Fig. 5(b). Firstly, note that the choice of end-contact work function renders the device unipolar, except at very low bias. Thus, the hole contribution to the transconductance at moderate and high V_{GS} is negligible. Secondly, it can be seen that g_m reaches a maximum, and then decreases as V_{GS} increases. This phenomenon has been reported elsewhere [12], [13]. The overall reduction in g_m at high V_{GS} relates to the increasing electron injection from the drain as the potential energy in the midlength region of the tube is reduced. The considerable structure in the transconductance plot is due to the presence of the quasi-bound states referred to earlier. As V_{GS} increases, the conduction band edge is pushed below the source Fermi level, and as the quasi-bound states cross this level, g_m increases. Thus, the situation is not dissimilar to that which gives rise to the peaks in capacitance. Indeed, at low temperatures, our simulations reveal that the peaks in transconductance and capacitance do occur at the same biases (see Fig. 6). Evidently, in going from $T = 4$ K to $T = 300$ K, thermal broadening causes peaks that are close together to merge, with the taller one dominating. Thus, the second peak in transconductance dominates the first, while the opposite is true in the capacitance case.

The changes in capacitance and transconductance discussed above lead to a very interesting and unusual bias dependence in the cutoff frequency f_T, as illustrated in Fig. 5(c). For the example of a 20-nm tube, as used here, f_T peaks at approximately 600 GHz. This is a long way from the value of 4 THz, which

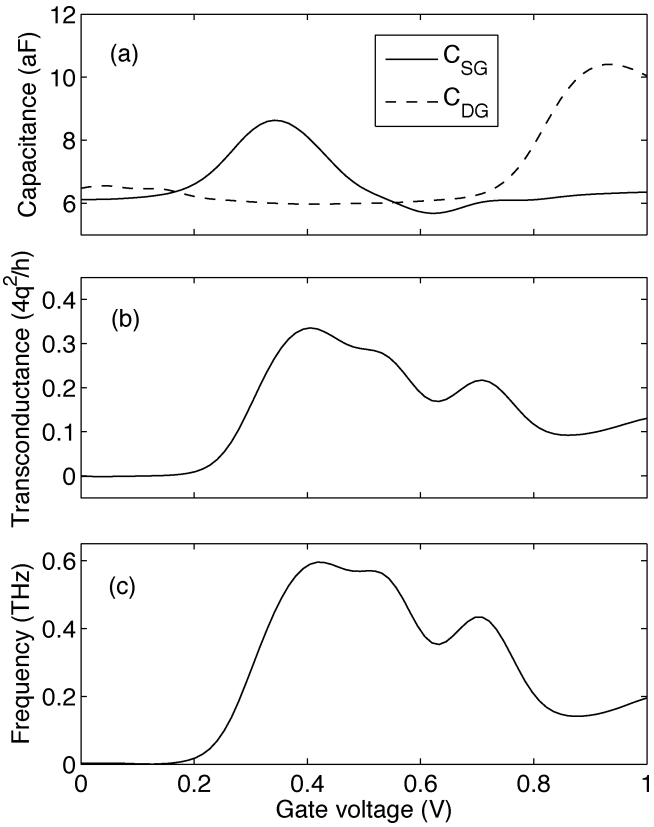

Fig. 5. f_T and its components. (a) The total capacitances associated with the source C_{SG} and with the drain C_{DG}. (b) Transconductance. (c) f_T.

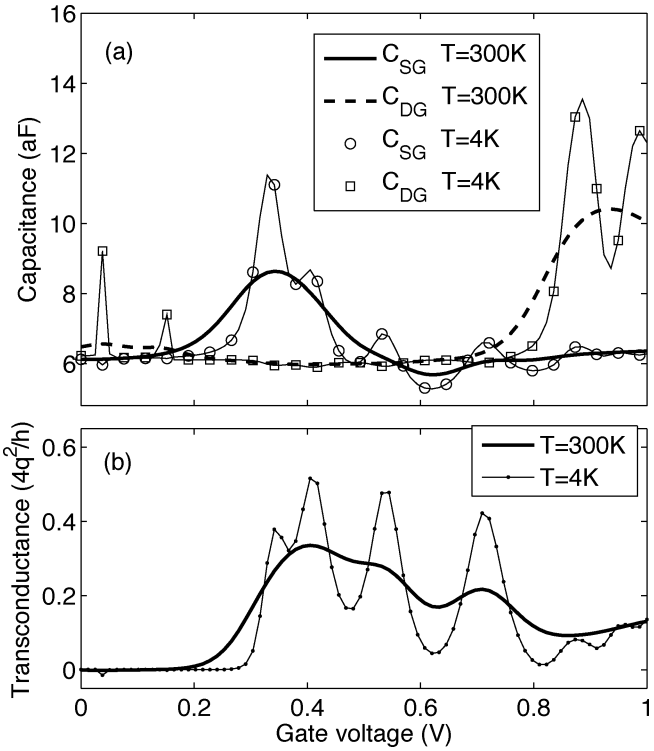

Fig. 6. Bias dependence at two temperatures for: (a) capacitance and (b) transconductance. Note that the peaks in transconductance coincide with peaks in capacitance at the lower temperature.

can be inferred from a recent model that ignored the bias dependence of the transconductance and capacitances, and attributed the device capacitance to that of an infinite coaxial system, with the quantum capacitance given by that of a metallic, rather than a semiconducting, nanotube [11]. In the finite coaxial system considered here, the midtube quantum capacitance is not explicitly identified, as it does not relate to the terminals on which the equivalent circuit is based. It is contained within C_{ST} and C_{DT}, the peak values of which turn out to have comparable magnitudes to the electrostatic electrode capacitances $C_{\rm SE}$ and $C_{\rm DE}$ in this particular example; thus, the overall capacitance shows significant bias dependence.

In future studies, we will attempt to optimize the Schottky-barrier CNFET as regards high-frequency performance. However, in concluding this paper, we can make a few comments regarding the parameters that are likely to be of importance. Clearly, the magnitude of the band discontinuity at the end contacts is significant. We have used a value of -5.5 eV for the depth of the metal conduction band below the Fermi level [9]. Higher values may be appropriate for noble metals of the type that appear suited to end contacts for CNFETs, in which case, one can expect more quantum mechanical reflection and a lower transconductance, leading to a reduced f_T. Increasing the barrier height by increasing the work function of the end-contact metal (in the case of n-type devices) will significantly degrade performance because of the appearance of a thick tunneling barrier in the ungated portion of the nanotube. Changing the nanotube to one of larger bandgap, yet maintaining the barrier height at approximately $-E_g/2$, may also degrade transconductance, at a given bias, because the ON current can be expected to be smaller, at least at low gate bias. Further, the peaks in transconductance and capacitance will be displaced to higher V_{GS} as more depressing of the conduction-band edge under the gate will be required to align the quasi-bound states with the source Fermi energy. Increasing the ungated regions L_{sg} and L_{dg} should be advantageous in a negative-barrier device because the electrostatic electrode capacitance will be reduced without a degradation in g_m. We have been quite aggressive in the vertical scaling of our device as we have used a high permittivity and a small thickness for the gate insulator. Relaxing these values will not change the resonances, but will shift the peaks in capacitance and transconductance to higher biases due to the poorer electrostatic coupling between gate and nanotube. Finally, we should mention that, in non-Schottky barrier CNFETs, in which the source and drain regions are formed by doping the ungated portions of the nanotube [20], [21], potential wells will form between the end contacts and the intrinsic gated part of the nanotube, and could lead to resonances somewhat similar to those described in this paper if the doped regions are short enough.

IV. Conclusions

From this study on ac small-signal simulations of Schottky-barrier CNFETs, it can be concluded that: 1) the generic small-signal equivalent-circuit model for field-effect transistors (FETs) is appropriate for studying the quasi-static ac performance of CNFETs provided the model parameters are rigorously derived; 2) in the case of short nanotubes with Schottky-barrier end contacts, a resonant structure is formed,

leading to the appearance of quasi-bound states; and 3) the quasi-bound states lead to gate-bias dependencies of the capacitances and transconductance, which, in turn, give rise to a short-circuit unity–current–gain frequency f_T, which displays a dependence on V_{GS} that is unusual in its oscillatory nature.

ACKNOWLEDGMENT

Author D. L. Pulfrey sincerely thanks Dr. S. Selberherr and Dr. E. Langer for enabling his appointment as a Guest Professor at the Institute of Microelectronics, Technical University of Vienna, Vienna, Austria, during the tenure of which this study was initiated.

REFERENCES

[1] K. David, "Silicon research at Intel," Intel Corporation, Hillsboro, OR, 2004. [Online]. Available: ftp://download.intel.com/research/silicon/Ken_David_GSF_030604.pdf.

[2] L. C. Castro, D. L. John, and D. L. Pulfrey, "Carbon nanotube transistors: an evaluation," in *Proc. SPIE Device and Process Technologies for MEM's, Microelectronics, and Photonics III Conf.*, vol. 5276, 2004. [Online]. Available: http://nano.ece.ubc.ca/pub/publications.htm, pp. 1–10.

[3] J. Guo, M. Lundstrom, and S. Datta, "Performance projections for ballistic carbon nanotube field-effect transistors," *Appl. Phys. Lett.*, vol. 80, no. 17, pp. 3192–3194, 2002.

[4] A. Javey, J. Guo, Q. Wang, M. Lundstrom, and H. Dai, "Ballistic carbon nanotube field-effect transistors," *Nature*, vol. 424, pp. 654–657, 2003.

[5] D. J. Frank and J. Appenzeller, "High-frequency response in carbon nanotube field-effect transistors," *IEEE Electron Device Lett.*, vol. 25, no. 1, pp. 34–36, Jan. 2004.

[6] J. Appenzeller and D. J. Frank, "Frequency dependent characterization of transport properties in carbon nanotube transistors," *Appl. Phys. Lett.*, vol. 84, no. 10, pp. 1771–1773, 2004.

[7] D. V. Singh, K. A. Jenkins, J. Appenzeller, D. Neumayer, A. Gill, and H.-S. P. Wong, "Frequency response of top-gated carbon nanotube field-effect transistors," *IEEE Trans. Nanotechnol.*, vol. 3, no. 3, pp. 383–387, Sep. 2004.

[8] X. Huo, M. Zhang, P. C. H. Chan, Q. Liang, and Z. K. Tang, "High frequency S parameters characterization of back-gate carbon nanotube field-effect transistors," in *Int. Electron Devices Meeting Tech. Dig.*, 2004, pp. 691–694.

[9] D. L. John, L. C. Castro, P. J. S. Pereira, and D. L. Pulfrey, "A Schrödinger–Poisson solver for modeling carbon nanotube FETs," in *Proc. NSTI Nanotechnology*, vol. 3, Mar. 2004. [Online]. Available: http://nano.ece.ubc.ca/pub/publications.htm, pp. 65–68.

[10] J. Guo, S. Datta, and M. Lundstrom, "A numerical study of scaling issues for Schottky-barrier carbon nanotube transistors," *IEEE Trans. Electron Devices*, vol. 51, no. 2, pp. 172–177, Feb. 2004.

[11] P. J. Burke, "AC performance of nanoelectronics: Toward a ballistic THz nanotube transistor," *Solid State Electron.*, vol. 48, pp. 1981–1986, 2004.

[12] L. C. Castro, D. L. John, and D. L. Pulfrey, "An improved evaluation of the DC performance of carbon nanotube field-effect transistors," *Smart Mater. Struct.*, Jul. 28, 2005., to be published.

[13] D. L. John, L. C. Castro, and D. L. Pulfrey, "Quantum capacitance in nanoscale device modeling," *J. Appl. Phys.*, vol. 96, no. 6, pp. 5180–5184, 2004.

[14] Y. P. Tsividis, *Operation and Modeling of the MOS Transistor*, 1st ed. New York: McGraw-Hill, 1988, ch. 9.

[15] S. Datta, *Electronic Transport in Mesoscopic Systems*. New York: Cambridge Univ. Press, 1995, vol. 3, Cambridge Studies in Semicond. Phys. Microelectron. Eng..

[16] W. Hönlein, F. Kreupl, G. S. Duesberg, A. P. Graham, M. Liebau, R. V. Seidel, and E. Unger, "Carbon nanotube applications in microelectronics," *IEEE Trans. Compon. Packag. Technol.*, vol. 27, no. 4, pp. 629–634, Dec. 2004.

[17] F. Léonard and J. Tersoff, "Dielectric response of semiconducting carbon nanotubes," *J. Appl. Phys.*, vol. 81, no. 25, pp. 4835–4837, 2002.

[18] A. Javey, H. Kim, M. Brink, Q. Wang, A. Ural, J. Guo, P. McIntyre, P. McEuen, M. Lundstrom, and H. Dai, "High-κ dielectrics for advanced carbon-nanotube transistors and logic gates," *Nature Mater.*, vol. 1, no. 4, pp. 241–246, 2002.

[19] E. Ungersboeck, M. Pourfath, H. Kosina, A. Gehring, B.-H. Cheong, W.-J. Park, and S. Selberherr, "Optimization of single-gate carbon-nanotube field-effect transistors," *IEEE Trans. Nanotechnol.*, vol. 4, no. 5, pp. 533–538, Sep. 2005.

[20] A. Javey, R. Tu, D. Farmer, J. Guo, R. Gordon, and H. Dai, "High performance n-type carbon nanotube field-effect transistors with chemically doped contacts," *Nano Lett.*, vol. 5, no. 2, pp. 345–348, 2005.

[21] Y.-M. Lin, J. Appenzeller, and P. Avouris, "Novel carbon nanotube FET design with tunable polarity," in *Int. Electron Devices Meeting Tech. Dig.*, 2004, pp. 687–690.

Leonardo C. Castro received the B.A.Sc. degree in electrical engineering from the University of British Columbia, Vancouver, BC, Canada, in 2001, and is currently working toward the Ph.D. degree in electrical engineering at the University of British Columbia.

His academic and research interests involve semiconductor device modeling, particularly its application to nanoelectronic devices.

D. L. John (S'01) received the B.A.Sc. (with honors) degree in engineering physics from the University of British Columbia (UBC), Vancouver, BC, Canada, in 2002, and is currently working toward the Ph.D. degree in electrical and computer engineering under the auspices of the Institute of Applied Mathematics at the University of British Columbia.

His research interests involve utilizing the techniques of applied mathematics for the modeling of emerging electronic devices.

D. L. Pulfrey (M'73–S'90–F'00) received the B.Sc. and Ph.D. degrees in electrical engineering from the University of Manchester, Manchester, U.K., in 1965 and 1968, respectively.

Since 1968, he has been on the faculty of the Electrical Engineering Department, University of British Columbia (UBC), Vancouver, BC, Canada. He has authored numerous papers, authored *Photovoltaic Power Generation* (New York: Van Nostrand, 1979) and coauthored *Introduction to Microelectronic Devices* (Englewood Cliffs, NJ: Prentice-Hall, 1989). His research area concerns semiconductor device modeling, currently with an emphasis on numerical analyses of and compact models for carbon nanotube transistors. He was previously involved with the development of models for metal–insulator–metal tunnel junctions, HBTs, photodetectors, and solar cells.

Dr. Pulfrey is a Fellow of the Canadian Academy of Engineering (2003). He was the inaugural recipient of the 1990 UBC Teaching Prize for Engineering.

Mahdi Pourfath was born in Tehran, Iran, in 1978. He received the Master of Science degree in electrical engineering from the Sharif University of Technology, Tehran, Iran, in 2002, and is currently working toward the Ph.D. degree at the Institute for Microelectronics, Technical University of Vienna, Vienna, Austria.

Since October 2003, he has been with the Institute for Microelectronics, Technical University of Vienna. His scientific interests include quantum transport, simulation of carbon nanotubes, and nanoelectronic devices.

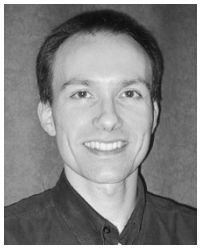

Andreas Gehring (M'04) was born in Mistelbach, Austria, in 1975. He received the Diploma degree and Ph.D. degree in electrical engineering from the Technical University Vienna, Vienna, Austria, in 2000 and 2003, respectively and the Diploma degree from the Vienna University of Economics and Business Administration, Vienna, Austria, in 2005.

In April 2000, he joined the Institute for Microelectronics, where he was a Research and Teaching Assistant from 2001 to 2005. He held visiting research positions with the Samsung Advanced Institute of Technology, Seoul, Korea, in the summer of 2001, at Cypress Semiconductor, San Jose, CA, in the summer of 2003, and at the Integrated Systems Laboratory, Eidgenössische Technische Hochschule (ETH) Zürich, Zürich, Switzerland, in the summer of 2004. Since March 2005, he has been with AMD Saxony, Dresden, Germany, where he is involved with low-leakage MOSFET device design.

Hans Kosina (S'89–M'93) received the Diplomingenieur degree in electrical engineering and Ph.D. degree from the Technical University of Vienna, Vienna, Austria, in 1987 and 1992, respectively.

For one year, he was with the Institute of Flexible Automation, Technical University of Vienna, and then joined then the Institute for Microelectronics, where he is currently an Associate Professor. In Summer 1993, he was a Visiting Scientist with the Advanced Product Research and Development Laboratory, Motorola Inc., Austin, TX. In Summer 1999, he was a member of visiting faculty with the Intel Corporation, Santa Clara, CA. His current research interests include device modeling of semiconductor devices, nanoelectronic devices, organic semiconductors and opto-electronic devices, development of novel Monte Carlo algorithms for classical and quantum transport problems, and computer-aided engineering in ULSI technology.

Dr. Kosina was the recipient of the 1998 Venia Docendi in microelectronics.